Molecular Mechanisms Mediating Antiangiogenic Action of the Urokinase Receptor-Derived Peptide UPARANT in Human Retinal Endothelial Cells

Carla Motta,[1] Gabriella Lupo,[2] Dario Rusciano,[3] Melania Olivieri,[3] Liliana Lista,[4] Mario De Rosa,[5] Vincenzo Pavone,[4] and Carmelina Daniela Anfuso[2]

[1]Bioos Italia Srl, Catania, Italy
[2]Department of Biomedical and Biotechnological Sciences, University of Catania, Catania, Italy
[3]Sooft Italia Spa, Roma, Italy
[4]Department of Chemical Science, University of Naples "Federico II" via Cintia, Italy
[5]Department of Experimental Medicine, Second University of Naples, Napoli, Italy.

Correspondence: Carmelina Daniela Anfuso, Department of Biomedical and Biotechnological Sciences, University of Catania, Biological Tower, via S. Sofia, 97, 95123 Catania, Italy; anfudan@unict.it.

CM and GL contributed equally to the work and should therefore be regarded as equivalent authors.

Submitted: May 11, 2016
Accepted: September 10, 2016

Citation: Motta C, Lupo G, Rusciano D, et al. Molecular mechanisms mediating antiangiogenic action of the urokinase receptor-derived peptide UPARANT in human retinal endothelial cells. *Invest Ophthalmol Vis Sci*. 2016;57:5723–5735. DOI:10.1167/iovs.16-19909

Purpose. To investigate the molecular mechanisms of the antiangiogenic activity of UPARANT, an antagonist of the urokinase-type plasminogen activator receptor (uPAR), on primary human retinal endothelial cells (HREC) as a model of in vitro angiogenesis.

Methods. The antiangiogenic activity of UPARANT was evaluated on endothelial cell migration, invasion, and tube formation. Human REC were further analyzed for viability, transendothelial electrical resistance (TEER), and tight junction (TJ) expression at the protein and mRNA levels. Vascular endothelial growth factor-related signaling molecules were also analyzed by Western and northern blots.

Results. UPARANT inhibited in a dose-dependent fashion HREC motility, invasion, and tube formation stimulated by VEGF-A, in a range of doses (1–100 nM) that had no effect on cell viability and proliferation. UPARANT also prevented the loss of permeability induced by VEGF-A, restoring normal TEER values and TJ protein expression. At the molecular level, UPARANT inhibited VEGFR-2 and STAT3 phosphorylation, thus decreasing VEGF and hypoxia-inducible factor 1-alpha expression, finally resulting in decreased activation of MEK/ERK, JNK, p38, and AKT signaling proteins.

Conclusions. These findings indicate that UPARANT exerts its antiangiogenic effects through the inhibition of the downstream signaling activated by angiogenic factors such as VEGF-A.

Keywords: angiogenesis, retina endothelial cells, migration, invasion, tubulogenesis, UPARANT

Neoangiogenesis is the physiological process of new blood vessel formation from pre-existing vessels; this is necessary to sustain the metabolism of growing cells, and is crucial for tissue healing and regeneration.[1] An imbalance of this process makes it become pathologic, contributing to disorders of an infectious, inflammatory, immune, and malignant nature.[2]

Aberrant retinal angiogenesis is a key component of several ophthalmic diseases that may lead to blindness. Proliferative diabetic retinopathy,[3–5] choroidal subretinal neovascularization,[6] and retinopathy of prematurity[7] are leading causes of blindness in the population worldwide. Neoplastic eye diseases, such as retinoblastoma, also appear to depend on angiogenic factors.[8] Therefore, finding a safer and more efficient antiangiogenic therapy is still a key challenge for the treatment of neovascular-dependent ocular pathologies.[9]

Vascular endothelial growth factor is the main regulator of angiogenesis, including retinal and choroidal angiogenesis.[10] Recent data from our laboratory have shown that human retinoblastoma cells in coculture with a primary human retinal endothelial cell line (HREC) derived from human retinal microvessels and pericytes release large amounts of VEGF-A.[11] Therapies based on anti-VEGF antibodies have been shown to improve visual outcome in patients with neovascular diseases.[12]

During new vessel formation, endothelial cells (EC) need to proliferate, migrate, and invade into the interstitial stroma using their proteolytic machinery, essential for the degradation of the extracellular matrix. For this reason, proteases and their receptors play a crucial role in angiogenesis. The urokinase-mediated plasminogen activation system (uPA) is a complex system of serine proteases involved in ECM degradation.[13] The receptor for urokinase-type plasminogen activator (uPAR) plays an important role in controlling cell migration[14,15] and uPAR signaling is closely related to angiogenesis.[16] In particular, it has been shown that the $uPAR_{88-92}$ sequence interacts with the formyl peptide receptors (FPR), inducing cell migration in an integrin-dependent manner.[17] In the retina uPAR is an important component of the angiogenic response; in mouse retinal neovascular pathology uPAR expression is upregulated in the microvessel endothelium.[18] Urokinase-type plasminogen activator is also expressed in bovine retinal EC and human retinal pigment epithelial cells, and its activation modulates their proliferation rate.[19] Moreover, inhibition of its activity prevents the blood–retinal barrier (BRB) breakdown in rodent

Investigative Ophthalmology & Visual Science

models of microvascular pathologies.[20,21] Whether uPAR inhibition may affect the permeability of HREC as a model of the BRB, remains to be investigated.

Based on these premises, and in the context of the research toward the setting up of antiangiogenic therapies based on the inhibition of endothelial cell migration, synthetic uPAR-peptide inhibitors for therapeutic applications have been developed.[21–23] Recently, Carriero et al.[24] have reported that the peptide Ac-L-Arg-Aib-L-Arg-L-α(Me)Phe-NH_2, named UPARANT, displays a remarkable resistance to enzymatic proteolysis. In vitro, the peptide inhibits tube formation by HUVEC; in vivo, following subcorneal implantation of pellets containing VEGF[24] and after intravitreal injections in mouse models of either oxygen-induced retinopathy[25] or choroidal neovascularization,[26] UPARANT significantly reduced the neovascular response, although the molecular mechanisms mediating these effects have not been clarified yet. To this purpose, in the present study we used an in vitro model of VEGF-A–driven angiogenesis in order to characterize the antiangiogenic activity of UPARANT in primary HREC cultures, in order to investigate the molecular mechanisms through which UPARANT exerts its antiangiogenic action.

Materials and Methods

Reagents and Antibodies

Recombinant human VEGF-A (VEGF-A_{165} isoform) was purchased from Peprotech (Rocky Hill, NJ, USA). UPARANT and control peptide ERFR were synthesized as previously described.[24] The serum-free endothelial cell basal medium (EBM) was purchased from Science Cell Research Laboratories (San Diego, CA, USA). Antibiotics, other reagents for cell culture, the SuperScript III first-strand synthesis system, Platinum PCR SuperMix and TrackIt were purchased from Invitrogen Life Technologies (Carlsbad, CA, USA). The protease inhibitor cocktail was obtained from Roche Applied Science (Indianapolis, IN, USA). The phosphatase inhibitor cocktail was purchased from Sigma-Aldrich Corp. (St. Louis, MO, USA). Polymerase chain reaction primer sets were purchased from Metabion International AG (Steinkirchen, Germany). All other chemicals were purchased from Sigma-Aldrich Corp.

A list of antibodies used in this study is shown in Supplementary Table S1.

Cell Culture

The primary HREC line was purchased from Innoprot (Elexalde Derio, Spain) and routinely fed with EBM supplemented with 5% fetal bovine serum (FBS), 1% endothelial cell growth supplement (ECGS), 100 U/mL penicillin, and 100 mg/mL streptomycin, also acquired by Innoprot. Human REC were used between the third and fifth in vitro passage. For experiments, cells were plated in complete culture medium to allow attachment; next, the culture medium was changed to EBM supplemented with 0.25% FBS plus factors (40–80 ng/mL VEGF-A, 1, 10, or 100 nM UPARANT), as appropriate for each experimental condition. For Western blot and RT-PCR analysis UPARANT was added 30 minutes before the addition of VEGF-A.

Cell Viability

Cell viability was assessed by the 3-[4,5-dimethylthiazol-2-yl]-2,5-diphenyl tetrasodium bromide (MTT) assay (Chemicon, Temecula, CA, USA), as previously described.[27] Cell number was determined by the Trypan blue exclusion test, followed by haemocytometer counting.[28] Cells failing to exclude the dye were considered not viable. Briefly, 5×10^3 HREC/well were seeded in 96-well plates, left to adhere in complete medium for 4 hours, rinsed twice with PBS, and then allowed to grow in EBM + 0.25% FBS with or without 40 ng/ml VEGF-A and/or different concentrations of UPARANT (1, 10, and 100 nM) for 72 hours at 37°C 5% CO_2. Culture medium was replaced every 24 hours. At the end of each time-point, HREC were incubated at 37 °C with MTT (0.5 mg/ml) for 4 hours; then 100 μL dimethyl sulfoxide was added and absorbance was measured at 570 nm in a plate reader (Synergy 2-bioTek; Perkin Elmer, Waltham, MA, USA).

Wound Healing Assay

To evaluate the effect of UPARANT on VEGF-A–induced HREC migration, a scratch-wound assay was used. Scratch wounds were created by scraping the cell monolayer with a 200-μl sterile tip. The wounded cultures were washed twice with PBS to remove detached cells and then treated with 80 ng/ml VEGF-A and/or different concentrations of UPARANT and control peptide ERFR (1, 10, and 100 nM) for 24 hours. The wound closure after treatment was monitored after 24 hours under an inverted Leica DM IRB microscope equipped with CCD camera (Leica-Microsystems, Wetzlar, Germany). The relative cell migration rate is calculated on the number of cells migrated into the wound area and expressed as percentage of untreated control. Quantitation of cell number was done on five different fields for each wound.

Cell Invasion Assay

To evaluate HREC invasion capability, transwells with a diameter pore size of 8.0 μm were coated with Matrigel (BD Biosciences, Erembodegem, Belgium) and inserted into a 24-well plate. Human REC (7×10^4 cells/well) were seeded in serum-free medium into the upper compartment. The lower compartment of the chamber was filled with 650 μL EBM with or without 80 ng/mL VEGF-A and/or 10 nM UPARANT. The inserts were incubated at 37°C for 24 hours and then removed from the plate. Nonmigrating cells on the upper surface of the filter were wiped with a cotton swab, and the filters stained for 30 minutes with a crystal violet solution (0.05% in 20% ethanol), then rinsed twice with distilled water and finally evaluated by light microscopy. Cells that had invaded the Matrigel and reached the lower surface of the filter were observed under a microscope at ×100 magnification. Five random nonoverlapping fields/well were photographed, and visible cells counted.

Tube Formation Assay

Fifty microliters of Matrigel were added to a 96-well plate and allowed to solidify at 37°C for 30 minutes. Human REC (1.5×10^4 cells/well) were treated in serum-free medium with or without 80 ng/mL VEGF-A and/or 10 nM UPARANT for 6 hours to allow the formation of tube-like structures. Pictures were taken using an inverted Leica DM IRB microscope equipped with a CCD camera. Tube length was measured using the Angiogenesis Analyzer tool for ImageJ software (http://imagej.nih.gov/ij/; provided in the public domain by the National Institutes of Health, Bethesda, MD, USA).

Transendothelial Electrical Resistance

To assess paracellular permeability of HREC as a model of BRB, TEER measurements were performed. TEER was measured with the Millicell-ERS system (MERS 000 01; Millipore AG, Volketswil, Switzerland). Inserts (Transwell, Corning, Inc.,

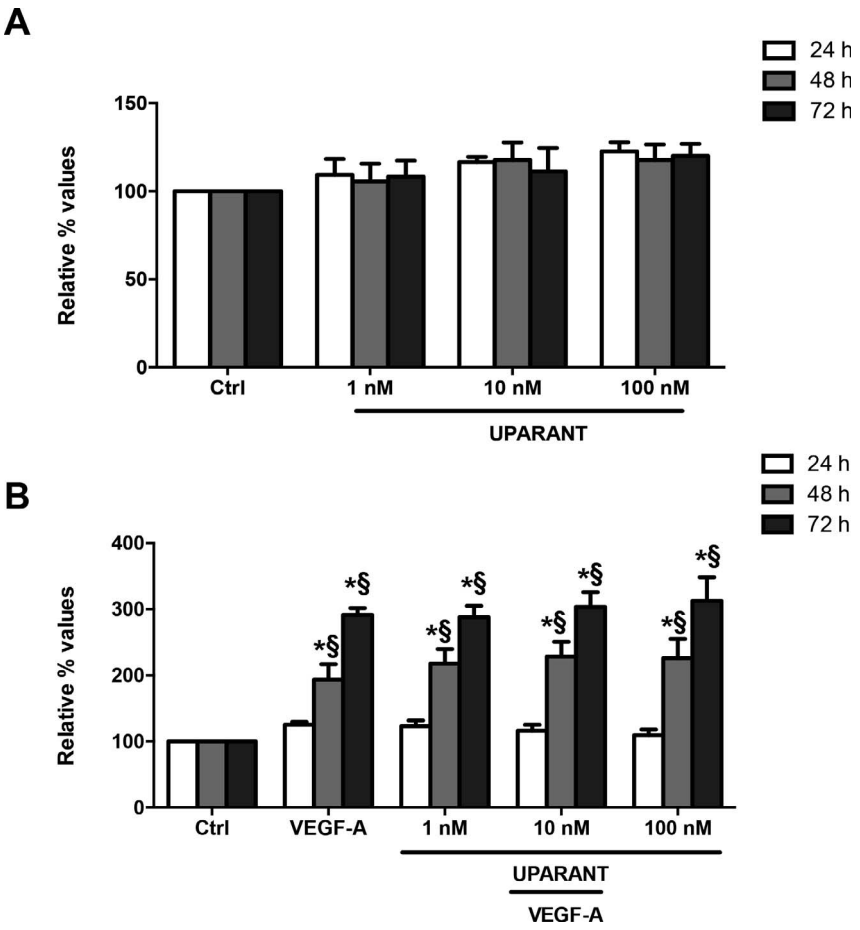

Figure 1. Vascular endothelial growth factor-A and UPARANT effects on HREC viability and growth. Human REC were allowed to grow in EBM + 0.25% FBS mixed with different concentrations of UPARANT (**A**) or with VEGF-A (40 ng/ml) plus or minus the same amounts of UPARANT (**B**) for 72 hours at 37°C and 5% CO_2. Cell viability and growth was estimated by the MTT assay, and reported as percentage of untreated control cells. Values are expressed as mean ± SD of three independent experiments, each involving six different wells per condition. *P* values were determined by 2-way ANOVA followed by Tukey's test (*$P < 0.05$ vs. respective controls, §$P < 0.05$ vs. preceding time).

Corning, NY, USA), were coated on the upper side with 1 μg/ml fibronectin. The coating was dried for 1 hour at 37°C, and rinsed twice with Ca^{2+}- and Mg^{2+}-free PBS before being placed in complete medium. Fibronectin-coated transwell inserts were used to measure the background resistance. Values are expressed as $\Omega \times cm^2$ and were calculated by the formula: (average resistance of experimental wells − average background resistance) × 0.33 (the area of the transwell membrane). TEER values were normalized to control wells without treatment. Human REC were plated on the upper side of the polycarbonate membrane (15×10^4 cells/well) of transwell inserts (24-well type, 3.0-μm pore size) and cultivated in complete medium for 3 days. Under these conditions the cells formed a confluent monolayer characterized by a stable TEER of approximately 40 $\Omega \times cm^2$. Prior to experiment with confluent HREC, the complete medium was replaced with serum-reduced medium and TEER was measured just before and then 24, 48, and 72 hours after the addition of 40 ng/mL VEGF-A and/or 1, 10, and 100 nM UPARANT, replacing the medium every day during the incubation period.

To evaluate TJ protein expression, HREC were incubated with EBM plus 0.25% FBS with 40 ng/mL VEGF-A, with or without 10 nM UPARANT for 3 days. The medium was replaced every 24 hours. After incubation, cell lysates were prepared as described below in the Western blotting section.

Western Blotting

Human REC in EBM plus 0.25% fetal calf serum (FCS) were preincubated with UPARANT or vehicle alone for 30 minutes, and then stimulated with VEGF-A (40 ng/mL) for the indicated times. At the end of each time-point, cells were detached by scraping, collected by centrifugation, and lysed as previously described.[29] After blotting, membranes were incubated overnight at 4°C with the primary antibodies listed in Supplementary Table S1, then 2 hours at room temperature with the specific secondary antibody, and immunocomplexes were finally detected by enhanced chemiluminescence (Amersham, Cologno Monzese, MI, Italy).

Total RNA Isolation and Semiquantitative RT-PCR

Total RNA was extracted from HREC by using the TRIzol reagent (Invitrogen Life Technologies, Monza, MB, Italy), reverse transcription of RNA was performed with the SuperScript III first-strand synthesis system according to the manufacturer's instructions. cDNA was amplified in a PX2 thermal cycler (Thermo Scientific Hybaid, Pittsburgh, PA, USA). Bands were made visible by UV-light and quantitated with the ImageJ software.

Primer sequences used for VEGF, VEGFR-2, hypoxia-inducible factor 1-alpha (HIF-1α), and β-actin are reported in Supplementary Table S2.

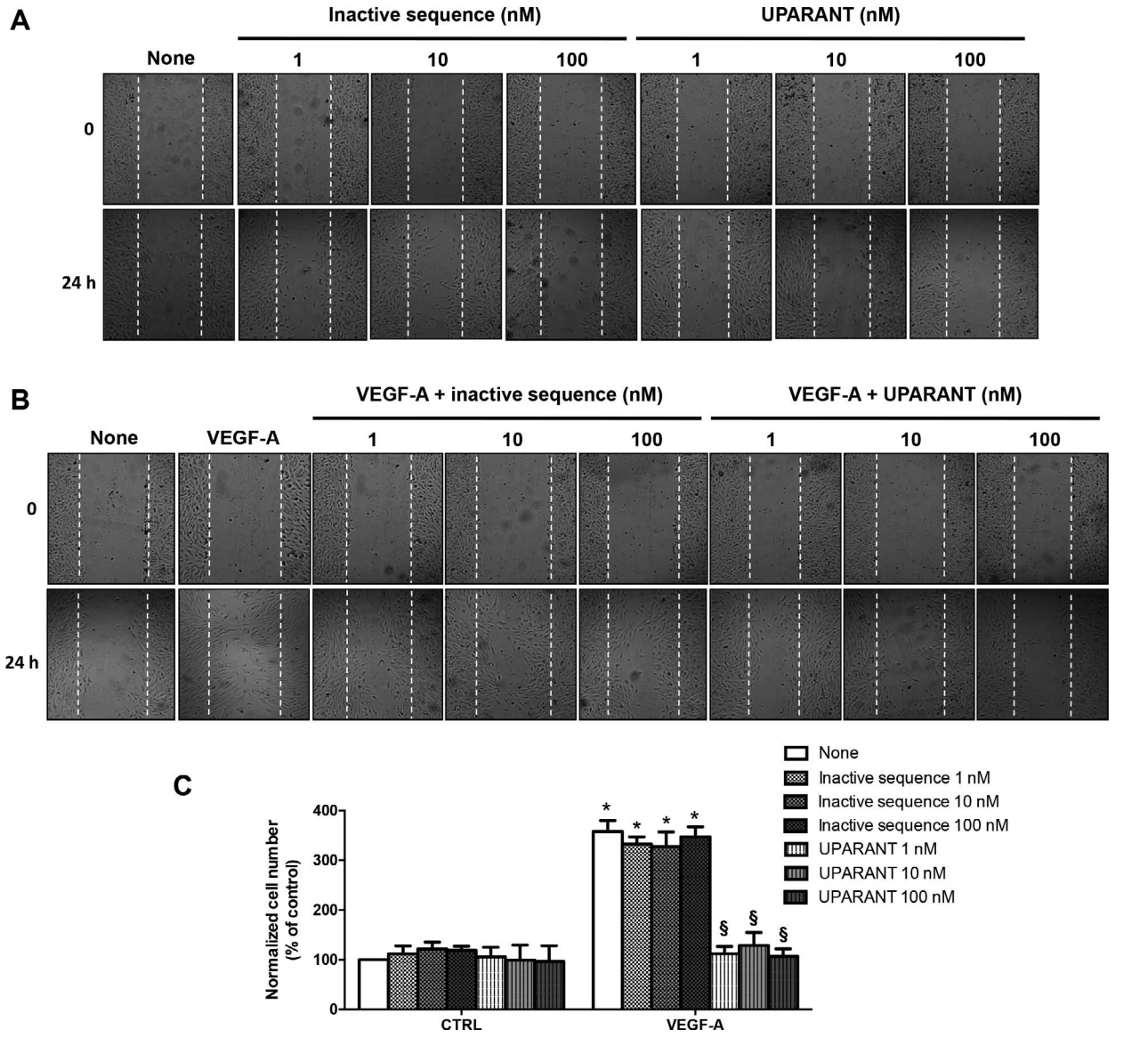

FIGURE 2. Vascular endothelial growth factor-A and UPARANT effects on HREC migration. Artificially wounded monolayers of confluent HREC were incubated for 24 hours with different concentrations of control peptide ERFR or UPARANT (**A**), or with 80 ng/ml VEGF-A with or without UPARANT or ERFR peptide at the indicated concentrations (**B**). Representative color-inverted photomicrographs of HREC cell migration are shown (magnification, ×40). The wounded area is indicated by *white dotted lines* (**C**). Quantitation of migrated cells was made with the aid of ImageJ software at five different areas for each wound. Data are the means ± SD from three independent wound healing assays, each one run in triplicate. Data were analyzed by 1-way ANOVA followed by Tukey's test (*$P < 0.05$ vs. respective control, §$P < 0.05$ vs. VEGF-A alone).

Antibody Arrays of Phosphorylated Receptor Tyrosine Kinase (p-RTK)

The Human Phospho-RTK Array Kit (catalogue no. ARY001B) was purchased from R&D System, Inc. (Minneapolis, MN, USA). Human REC were treated with 10 nM UPARANT for 30 minutes, with 40 ng/mL VEGF-A for 15 minutes, or with a combination of the two (UPARANT 30 minutes, plus VEGF-A 15 minutes), and cell lysates prepared according to manufacturer's instructions. Phosphorylated receptor tyrosine kinase array membranes were then incubated overnight at 4°C with 2 mL of each cell lysate containing equal amounts of protein. The membranes were incubated with anti-phospho-tyrosine-HRP antibody for 2 hours at room temperature, and the immunocomplexes in each array membrane were detected by the enhanced chemiluminescence reagent. Densities of immunoreactive spots were quantitated with the ImageJ software. Results are shown in Supplementary Figure S1.

Statistical Analysis

Statistical significance between two groups was analyzed by Student's *t*-test. One-way ANOVA, followed by Tukey's post hoc test, was used for multiple comparisons. *P* values less than 0.05 were considered statistically significant.

RESULTS

Human REC represent an ideal cell model system to study the molecular mechanisms of UPARANT effects on retinal neoangiogenesis. In the first part of this work, we investigated whether UPARANT could inhibit the response of this cell line

to VEGF-A–induced in vitro angiogenesis; in the second part we will illustrate how the signal transduction downstream VEGF-A stimulation is influenced by UPARANT.

UPARANT Does Not Interfere With Cell Viability and Proliferation

The effect of UPARANT at 1, 10, 100 nM on HREC viability and proliferation was evaluated by the MTT assay (Fig. 1). The presence of VEGF-A at 40 ng/mL concentration induced an expected increase of cell proliferation (1.93- and 2.71-fold at 48 and 72 hours, respectively, $P < 0.05$: Fig. 1B), whereas UPARANT by itself did not affect cell viability or proliferation at any of the tested doses (Fig. 1A), nor did it interfere with VEGF-A stimulation of proliferation (Fig. 1B).

UPARANT Decreases VEGF-Induced Migration and Invasion

To study the effect of UPARANT on VEGF-A–induced cell migration and invasion, experiments were performed following two different procedures.

Migration was evaluated by the artificial wound-healing assay (Fig. 2). Contrast phase representative photographs show HREC cultures after wounding of the monolayer and the wound edge advancement after 24 hours incubation with control inactive peptide ERFR,[24] UPARANT alone (both, no effect: Fig. 2A), and VEGF-A in the absence or in the presence of 1, 10, and 100 nM UPARANT (Fig. 2B). The quantitative representation of the results is shown in Figure 2C. Vascular endothelial growth factor-A improved HREC wound closure by 2-fold at 24 hours ($P < 0.05$). UPARANT at 10 and 100 nM significantly counteracted the effect of VEGF-A, and decreased wound closure by roughly 30% ($P < 0.05$). As expected, control tetrapeptide ERFR was ineffective.

In a second set of experiments, invasion of HREC through Matrigel-coated transwell membranes was induced by the presence of VEGF-A ± 10 nM UPARANT in the lower well (Fig. 3). After 24 hours VEGF-A caused a significant 6.6-fold increase ($P < 0.05$) in the number of cells crossing the filter as evaluated by manually cell count (Fig. 3B). Conversely, 10 nM UPARANT caused a 40% reduction of such invasion ($P < 0.05$) (Fig. 3B).

UPARANT Reduces VEGF-A–Stimulated Neovessel Tube Formation

Representative optical contrast phase micrographs of cell-to-cell interaction and organization on Matrigel are shown in Figure 4A. Human REC plated onto Matrigel under control conditions adhered in a short time and expressed their typical elongated phenotype very quickly, within 6 hours of incubation (Fig. 4A, panel a). The cells emitted long offshoots from the cell bodies (white arrows) creating physical contact, necessary for recognition and spatial organization. The presence of VEGF-A strongly enhanced these morphologic changes (Fig. 4A, panel b): many more cells than in the control wells established a higher number of reciprocal contacts. UPARANT alone at 10 nM had no influence on the morphology of HREC on Matrigel (Fig. 4A, panel c), whereas it prevented the stimulatory effects of VEGF (Fig. 4A, panel d). Tube formation under all culture conditions was quantitated by counting tubule branch points, defined as cell intersections containing at least three tubules, namely parts of the tube skeleton where three or more tubes converge (Fig. 4B). Vascular endothelial growth factor-A induced an increase of branching points by 3.9-fold ($P < 0.05$) compared with control and to UPARANT alone-treated cells. The addition of UPARANT

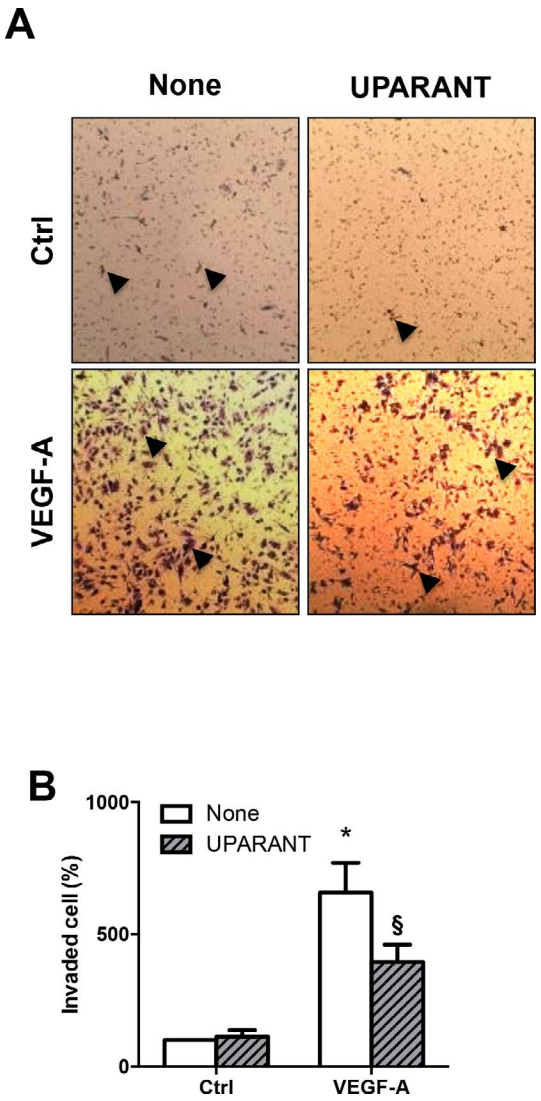

FIGURE 3. Vascular endothelial growth factor-A and UPARANT effects on HREC invasion. Matrigel-coated filters with 8-μm pores were fixed and noninvading cells on the upper filter side removed with a cotton swab. Invading cells on the bottom side of the filter were evaluated after crystal violet staining by light microscopy. Representative fields are shown at ×100 magnification (**A**). Human REC migration was quantitated in triplicate membranes by counting the cells in five different fields of each membrane (**B**). Data are the means ± SD of three independent experiments, analyzed by 1-way ANOVA followed by Tukey's test (*$P < 0.05$ vs. control, §$P < 0.05$ vs. VEGF-A alone).

10 nM to VEGF-treated cells reduced branching by 50.4% ($P < 0.05$) (Fig. 4B), in good correlation with the measurement of tube length (Fig. 4C).

UPARANT Prevents VEGF-A–Induced HREC Monolayer Permeability

The formation of a continuous, impermeable cell monolayer on the upper surface of a transwell chamber results in a strong detectable increase of the TEER measured between the upper and the lower compartments of the chamber. The impermeability of such monolayer is due to the sealing of endothelial cells via formation of TJ. The exposure of HREC monolayers to different concentrations (1–100 nM) of UPARANT alone had no effect on TEER, whereas VEGF-A treatment (40 ng/mL) disrupted the monolayer integrity, causing a significant, time-

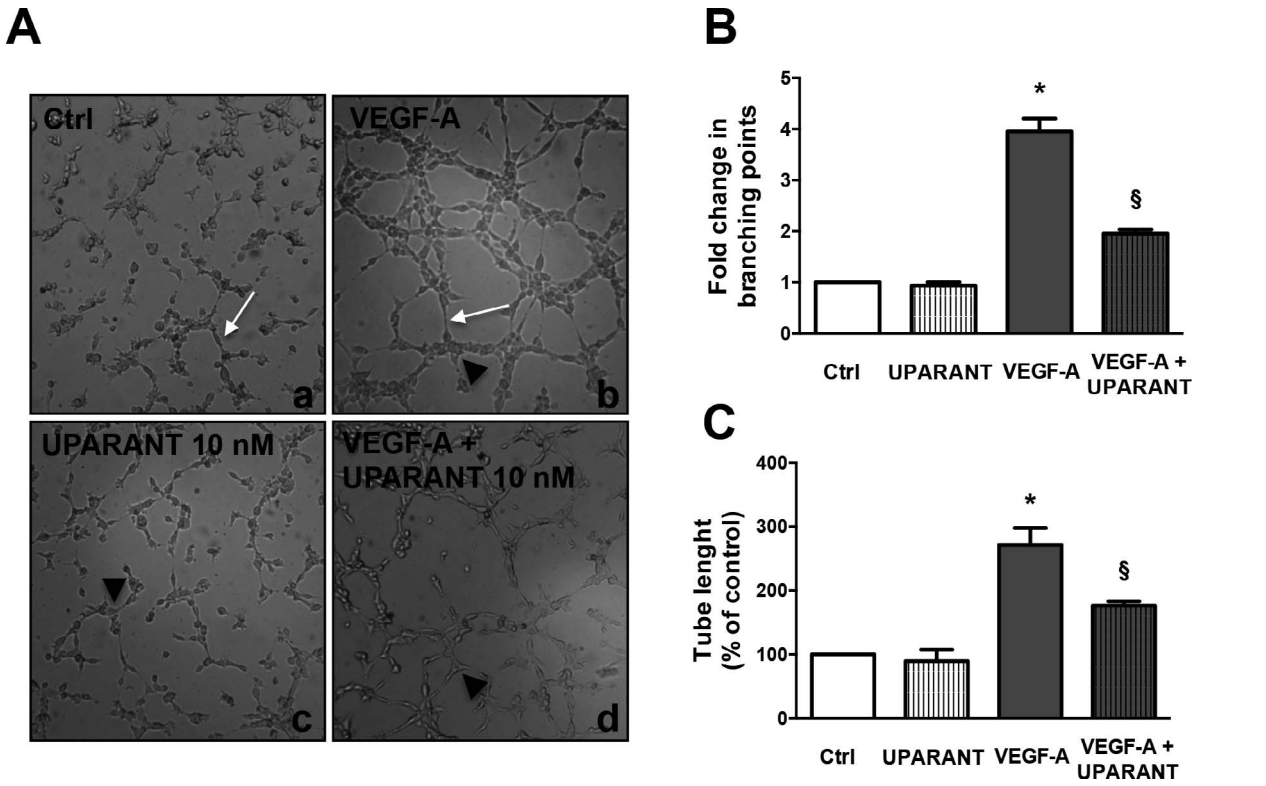

FIGURE 4. Vascular endothelial growth factor-A and UPARANT effects on HREC morphogenesis. Endothelial tube formation was evaluated by light microscopy in terms of branching points and tube length. Representative fields are shown at ×100 magnification (**A**). Branching points (*arrowheads*) folds change is shown with respect to cells seeded in the absence of VEGF (**B**). Tube elongation was calculated with respect to cells grown in the absence of VEGF (**C**). *White arrows* indicate long offshoots emitted from cell bodies. Values are expressed as mean ± SD of three independent experiments performed in duplicate wells. *P* values were determined by 1-way ANOVA followed by Tukey's test (*$P < 0.05$ vs. control, §$P < 0.05$ vs. VEGF-A).

dependent decrease of TEER by 32%, 45%, and 39% at day 1, 2, and 3, respectively ($P < 0.05$) (Fig. 5A). Such a decrease of TEER induced by VEGF-A was partially prevented by UPARANT at 1 nM (28%, 22%, and 8% observed decrease at day 1, 2, and 3, respectively, $P < 0.05$), and completely prevented at the higher concentrations of 10 and 100 nM (Fig. 5B).

In a separate experiment the expression of TJ proteins was evaluated on HREC monolayers after 24 hours of treatment with VEGF-A (40 ng/ml) in the presence or absence of 10 nM UPARANT. Tight junction protein expression was strongly inhibited by incubation with VEGF-A, which decreased claudin-1, claudin-5, and occludin amounts by 65%, 85%, and 60%, respectively ($P < 0.05$), correlating well with the loss of TEER. UPARANT at 10 nM significantly prevented the decrease of TJ protein expression: claudin-1 level returned similar to untreated control cells, whereas the observed decrease for claudin-5 and occludin were respectively 55% and 33% ($P < 0.05$) (Figs. 5C, 5D).

UPARANT Reduces VEGF-A Expression and VEGFR-2 Expression/Activation

Experiments were performed to investigate the possible involvement of UPARANT in regulating the level of VEGF-A and the level and activation (by phosphorylation) of its cognate receptor VEGFR-2 (Fig. 6).

Vascular epithelial growth factor-A stimulation of HREC (Fig. 6A) for 5 and 30 minutes triggered VEGFR-2 phosphorylation by almost a 2.0- and 1.45-fold increase ($P < 0.05$), respectively; receptor activation was almost back to control level after 60 minutes of incubation. The simultaneous presence of UPARANT at 10 nM and VEGF-A partially inhibited VEGFR-2 phosphorylation at 5 minutes (1.25-fold increase over control: 37.5% inhibition, $P < 0.05$), bringing it back to control levels already at 30 minutes. The expression level of VEGFR-2 remained stable (Fig. 6A). By using a human phospho-RTK array kit we also screened HREC for the activation of other 49 tyrosine kinase receptors: the only growth factor phosphorylated after VEGF-A addition was VEGFR-2 (25-fold increase, $P < 0.05$). UPARANT (10 nM) coincubated with VEGF reduced VEGFR-2 phosphorylation level by almost 37% ($P < 0.05$), without inducing, by itself, any other receptor phosphorylation (see Supplementary Fig. S1).

The mRNA level of VEGFR-2 showed no variation between 1 and 4 hours, either in the presence of VEGF-A alone, or in the concomitant presence of UPARANT (Fig. 6B).

Vascular endothelial growth factor-A incubation for 24 hours stimulated its own levels by almost 3.3-fold ($P < 0.05$), due to the presence of a known autocrine loop,[30–32] and was drastically reduced by 64% ($P < 0.05$) when UPARANT at 10 nM was simultaneously present (Fig. 6C). Accordingly, after incubation with VEGF-A for 1, 2, and 4 hours, VEGF-A-mRNA substantially increased by 5.3-, 5.2-, and 6.0-fold, respectively ($P < 0.05$). The concomitant presence of 10 nM UPARANT decreased such a response by 30%, 37%, and 77%, respectively ($P < 0.05$) (Fig. 6D).

UPARANT Affects the Signalling Pathways Triggered by VEGF-A

The putative role of UPARANT on proteins involved in intracellular signaling of VEGF-A was investigated in HREC by

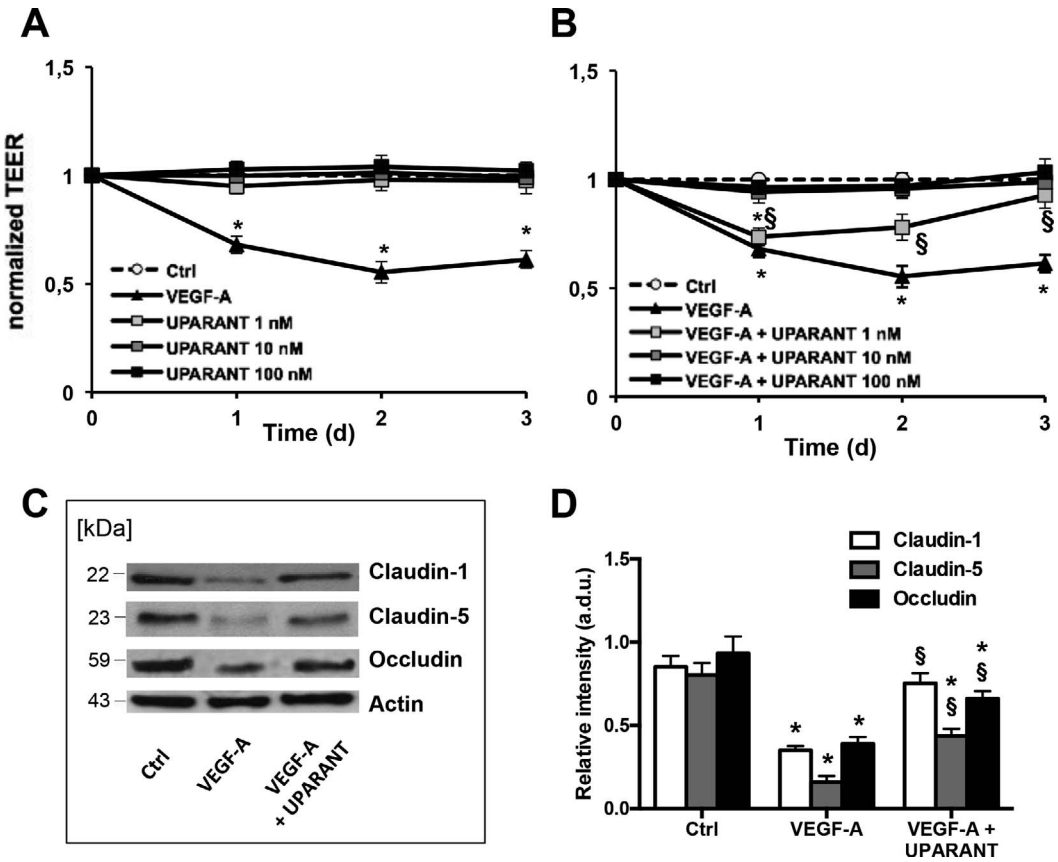

FIGURE 5. Vascular endothelial growth factor-A and UPARANT effects on TEER and TJs protein expression. TEER was measured in triplicate wells at the indicated time points after: (**A**). Treatment of confluent HREC with 40 ng/ml VEGF-A or with different concentrations of UPARANT; (**B**). Treatment of confluent HREC with 40 ng/ml VEGF-A with or without different concentrations of UPARANT. (**C**) Representative Western blot of TJ protein expression after VEGF-A treatment for 1 day with or without 10 nM UPARANT. (**D**) Bar graphs (in arbitrary densitometric units, a.d.u.) representing the means ± SD from three independent experiments. *P* values were determined by 2-way ANOVA followed by Tukey's test (*$P < 0.05$ vs. control, §$P < 0.05$ vs. VEGF-A).

checking the expression/activation levels of AKT, JNK, p38, and ERK, known for transducing migration and survival signals in EC.[33] Phosphorylation levels of these proteins were measured after 5, 30, and 60 minutes of VEGF-A induction. Figure 7A shows the immunoblot detection of total and phosphorylated proteins; the respective quantification is reported in Figures 7B through 7E, showing the phosphorylated/total proteins ratio of densitometric values. Vascular endothelial growth factor-A–stimulated activation peaked at 5 minutes of incubation (2.03-, 3.07-, 2.06-, 9.78-fold increase for AKT, JNK, p-38, ERK 1/2, respectively, $P < 0.05$), then declined at remaining incubation times. The presence of 10 nM UPARANT caused a significant reduction of the phosphorylation levels in all proteins at 30 and 60 minutes, returning them almost to baseline levels. JNK and p38 activation was completely prevented already at 5 minutes. These results indicate that UPARANT may inhibit HREC migration, invasion, and tube formation by affecting the downstream cascade of MEK/ERK, MEK/JNK, PI3-K/p38, and PI3-K/AKT pathways.

UPARANT Reduces STAT3 and HIF-1α Expression

STAT3 and HIF-1α are two known key regulators in VEGF signal transduction and angiogenic response (Labazi M, et al. *IOVS* 2009;50:ARVO E-Abstract 2942).[34] Incubation of HREC with VEGF-A caused a drastic increase in STAT3 phosphorylation by 3.3-fold at 30 and 60 minutes ($P < 0.05$), without changing the level of protein expression. The presence of 10 nM UPARANT prevented such an increase, maintaining the values close to those found in untreated cells (Fig. 8A). STAT3 activation in retinal EC is known to increase their expression of HIF-1α.[35] Accordingly, after 1 to 4 hours stimulation with VEGF-A, HIF-1α transcription level increased between 3- and 4-fold ($P < 0.05$) (Fig. 8B). The effect of UPARANT at 10 nM on this induction was dramatic, and already at 1 hour the expression level of HIF-1α mRNA was back to the control level, remaining stable until 4 hours of treatment.

DISCUSSION

Abnormal angiogenesis is among the causes of several pathologies in which an ischemic insult triggers an overproduction of angiogenic factors that alter the normal vascularization process. Retinal diseases, such as proliferative diabetic retinopathy, neovascular AMD, and retinopathy of the prematurity represent a class of such pathologies, very often leading to visual loss in affected patients. Vascular epithelial growth factor is the main angiogenic factor regulating vascularization of the retina and the choroid[10]; therefore, the predominant therapeutic approach to these kinds of diseases is nowadays based on drugs that prevent its binding to cognate receptors.[36]

In this paper, we show that a different therapeutic approach could be possible, in which the target is the downstream signaling triggered by VEGFR-2 activation.

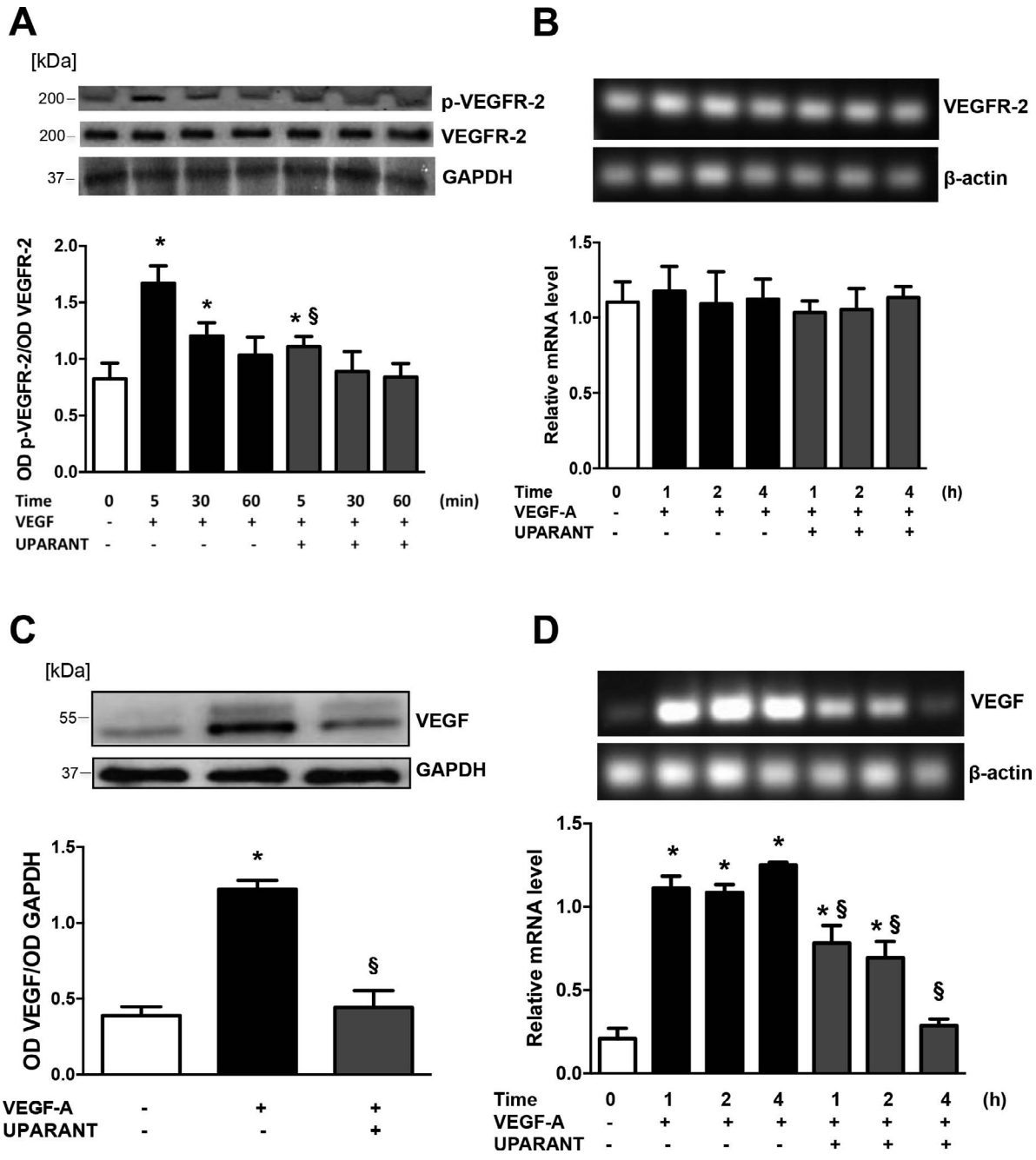

Figure 6. UPARANT effects on VEGFR-2 activation and VEGF-A expression. Vascular endothelial growth factor receptor-2 phosphorylation and protein expression (**A**), or VEGFR-2 transcription (**B**) were assessed respectively by Western blot analysis or RT-PCR in control HREC (no treatment) or HREC pretreated with 10 nM UPARANT for 30 minutes and then treated with 40 ng/ml VEGF-A at the indicated time points. Results are expressed as the ratio over total VEGFR-2 ([**A**] *bottom panel*) or β-actin mRNA ([**B**] *bottom panel*). Vascular endothelial growth factor protein expression (**C**) was assessed by Western blot analysis in control HREC (no treatment) or HREC treated for 24 hours with VEGF-A (40 ng/ml) plus or minus 10 nM UPARANT. Results are expressed as the ratio to glyceraldehyde 3-phosphate dehydrogenase (GAPDH; [**C**] *bottom panel*). Vascular endothelial growth factor-A transcription rate (**D**) was assessed by RT-PCR in control HREC (no treatment) or HREC pretreated with 10 nM UPARANT for 30 minutes and then treated with 40 ng/ml VEGF-A at the indicated time-points. Results are expressed as the ratio to GAPDH ([**D**] *bottom panel*). Data represent the means ± SD from three independent experiments (*$P < 0.05$ vs. control, §$P < 0.05$ vs. VEGF-A same time; 1-way ANOVA, followed by Tukey's test).

UPARANT is a synthetic peptide antagonizing the uPA receptor, thus inhibiting its interactions with the other cellular partners required to induce the invasive phenotype of microvascular EC, necessary for angiogenesis. Urokinase-type plasminogen activator receptor is a Glycosylphosphatidylinositol (GPI)-anchored receptor that takes part in the regulation of a wide range of cellular events, such as motility, invasion, and gene expression. Because it lacks an intracellular domain, uPAR exerts its activity by forming supramolecular complexes with other cell membrane receptors, activating a downstream signaling through mediators such as FAK, Src, Rac, Ras/Raf ERK/MAPK, and JAK/STAT.[14] The assembly of uPAR in composite regulatory units with αvβ3 integrins and the formyl peptide receptor (FPR) has been shown.[21] Activation of FPR

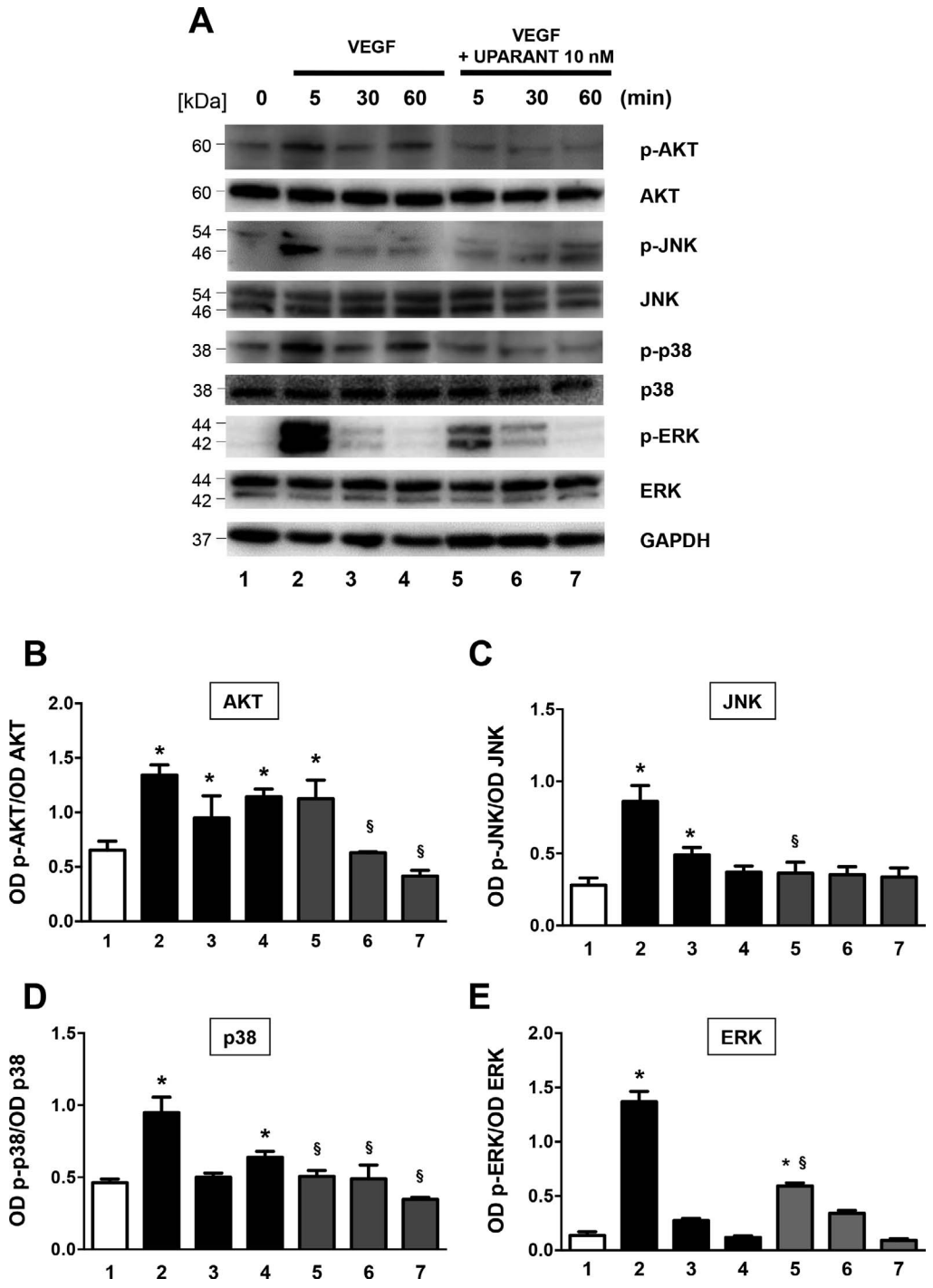

Figure 7. UPARANT effects on signal transduction induced by VEGF-A. Expression of MAPKs in control HREC (no treatment) or HREC pretreated with 10 nM UPARANT for 30 minutes and then treated with 40 ng/ml VEGF-A at the indicated times. A representative blot is shown for AKT, JNK, p38, and ERK, phosphorylated, and total expression. (**B**–**E**) Densitometry analysis of phosphorylated/total protein ratio of each band (a.d.u.). Data represent the means ± SD from three independent experiments. *P* values were determined by 1-way ANOVA followed by Tukey's test (*$P < 0.05$ vs. control, §$P < 0.05$ vs. VEGF-A same time-point).

may in turn activate STAT3 and HIF-1α signaling pathways, controlling angiogenesis and inflammation.[37] There is a demonstrated interaction between uPAR and VEGFR-2, that leads to a redistribution of uPAR on the cell membrane, resulting in its accumulation at the invasive leading edge of EC,[38] where uPAR controls integrin-dependent cell migration, interacting with the fibronectin and vitronectin integrin receptors α3β1/α5β1 and αvβ5/αvβ3.[39] Pro-urokinase (pro-uPA) is also activated leading to the further activation of proMMP-2 and more pro-uPA. Urokinase-type plasminogen activator receptor is finally internalized via an low density lipoprotein receptor-like molecule.[40] This VEGF-induced pro-uPA activation on EC might be one of the initial steps in matrix degradation during the angiogenic process.[41]

Consistent with these mechanisms, we have shown here that UPARANT does not influence HREC growth or its stimulation by VEGF-A, indicating that VEGFR-2 and the growth signaling are not the main targets of UPARANT.

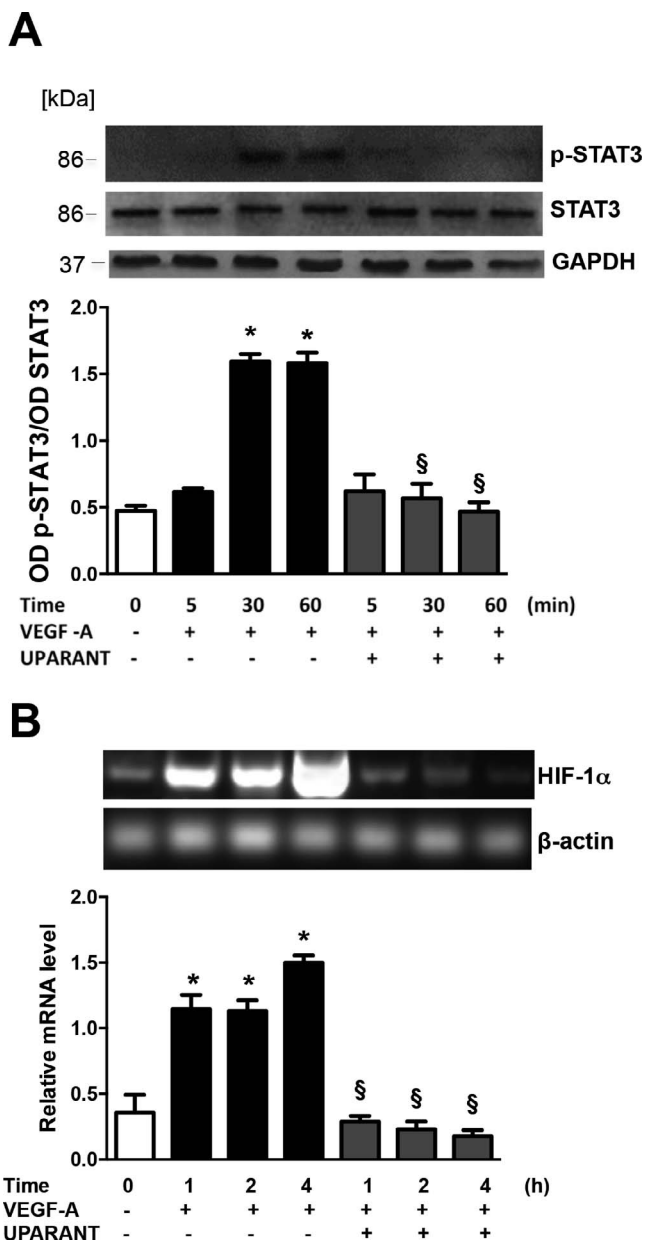

FIGURE 8. Vascular endothelial growth factor-A and UPARANT effects on STAT3 and HIF-1α. Western blot of STAT3 activation by phosphorylation and total STAT3 protein expression ([**A**] *upper panel*). Densitometric quantitation of p-STAT3 normalized to the level of total STAT3 ([**A**] *lower panel*). HIF-1α mRNA expression evaluated by RT-PCR (**B**, *upper panel*). Densitometric quantitation of HIF-1α mRNA normalized to the level of control β-actin ([**B**] *lower panel*). Data represent the means ± SD from three independent experiments. *P* values were determined by 1-way ANOVA followed by Tukey's test (*$P < 0.05$ vs. control, §$P < 0.05$ vs. VEGF-A same time-point).

Vascular endothelial growth factor-A treatment of HREC triggers activation of only VEGFR-2; none of the other 39 tyrosine-kinase receptors investigated (including VEGFR-1 and –3) appeared to be activated (Supplementary Fig. S1). However, UPARANT in each of the two experiments evaluating its effects on VEGFR-2 activation (Fig. 6, Supplementary Fig. S1) exerted only 37% inhibition of VEGFR-2 activation by VEGF-A, and this might suggest that such a partial inhibition is not sufficient to inhibit cell growth, which directly depends on VEGFR-2 activation.[42]

On the contrary, VEGF-A–induced cell motility, invasion, and microvascular tube formation were all inhibited in a dose-dependent fashion by UPARANT. This was also accompanied by a restoration of the EC permeability barrier, disintegrated by VEGF-A treatment. In the motility, morphogenesis, and invasion assays UPARANT was able to counteract even the highest concentration of VEGF-A used (80 ng /ml).

Vascular endothelial growth factor is known to induce its own biosynthesis through an autocrine stimulation process requiring the activation of the STAT3 transcription factor.[43] UPARANT disrupts this process, interfering with the activation of VEGFR-2, STAT3, and the transcription of HIF-1α, finally resulting in a decreased VEGF biosynthesis.[44] The STAT3 cytoplasmic transcription factor is known to be activated by a number of oncogenes, cytokines, and growth factors, and to participate in different signal pathways depending on the cell types.[45] STAT3 is phosphorylated/activated in a wide variety of cancers and its activation increases both tumor angiogenesis and VEGF expression.[46] Activation of STAT3 is indeed considered a biomarker of VEGF-mediated endothelial activation.[47] In a representative model of human retinopathy of prematurity, NOX4 regulated VEGFR-2-mediated neovascularization through STAT3 activation.[48]

The activated VEGFR-2 may interact with integrins, uPAR, and FPR (Fig. 9), thus modulating cell adhesion, motility, and invasion through the activation of: (1) AKT and p38 MAPK, responsible for actin reorganization, motility, and tube formation[49]; and (2) JNK and ERK1/2 that regulate MMP expression, invasion, and morphogenesis.[50,51] The interference of UPARANT with the formation of the above supramolecular complex prevents VEGF-mediated activation of AKT, JNK, p38 MAPK, and ERK, likely leading to the observed inhibition of motility, invasion, and tube formation in HREC. Moreover, in bovine retinal EC stimulated by VEGF, uPAR activation led to the engagement of the p38/β-catenin complex, resulting in increased paracellular permeability.[52] Accordingly, our data show that UPARANT, likely through the inhibition of p38 MAPK activation, prevents the loss of impermeability of the endothelial monolayer induced by VEGF-A, and increases TJ protein expression.

CONCLUSIONS

Data presented in this paper give a better understanding, at the molecular level, of the antiangiogenic effect of UPARANT demonstrated in vivo in mouse models of retinopathy of prematurity (ROP)[25] and choroidal neovascularization (CNV).[26] In fact, in this in vitro model system of retinal neoangiogenesis with HREC, UPARANT inhibited the cell signaling triggered by VEGF-A stimulation, thus inhibiting their response in terms of cell motility, invasion, and morphogenesis, and restored the endothelial barrier accordingly to what observed also in vivo.[25,26]

UPARANT is therefore the prototype of a new class of antiangiogenic molecules that target the angiogenic cascade downstream of the activation of the main angiogenic receptor, VEGFR-2. Hence, it could be expected that this class of angiogenesis inhibitors has a broader efficacy with respect to the anti-VEGF approach that is today predominant, which is, by definition, limited only to the angiogenesis promoted by VEGF induction. In fact, in a recent publication, it was shown that UPARANT can inhibit the angiogenic response of human umbilical vein endothelial cells (HUVEC) stimulated by either VEGF or by the vitreous body of retinopathic patients, likely containing a wider array of growth and angiogenic factors than VEGF alone.[25] Thus, bearing in mind the evidence presented in this paper and what has already been published on mouse

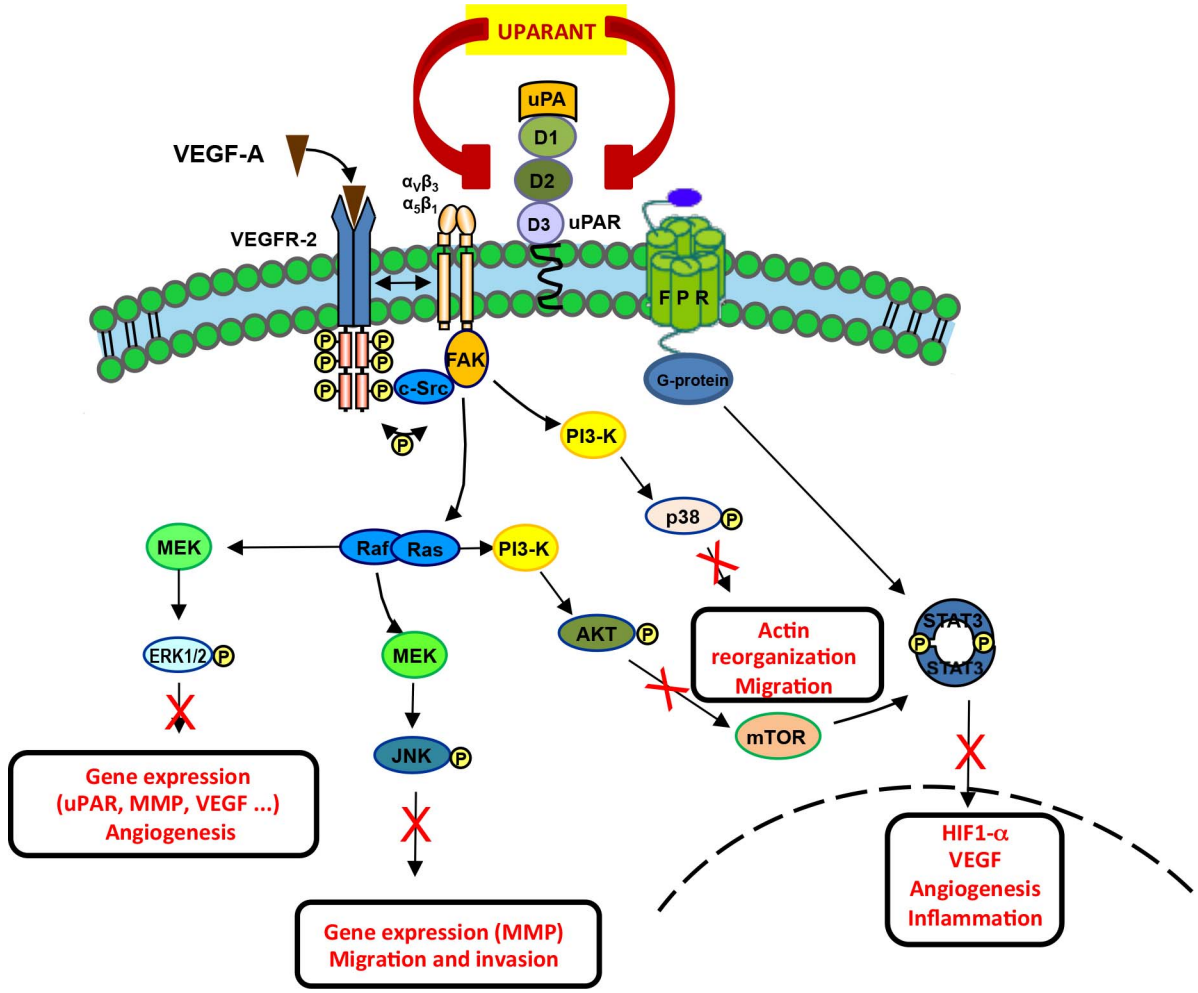

FIGURE 9. UPARANT inhibition of the angiogenic events induced by VEGF-A. In the proposed model, UPARANT inhibits the formation of the uPAR/integrin/FPR complex stimulated by VEGFR2 activation, and its downstream cascade of events, finally leading to inhibition of activation of ERK1/2, JNK, p38, and AKT on the one hand, STAT3 and HIF-1α on the other, therefore impinging on migration, invasion and morphogenesis of HREC.

model systems,[25,26] UPARANT could be considered a promising new molecule that might be able to treat retinal neovascular diseases, either alone, or in association with some of the available anti-VEGF products.

Acknowledgments

The authors thank Paola Bagnoli and Massimo Dal Monte (University of Pisa, Italy) for their critical reading of the manuscript, and English proofreading by Antony Bridgewood (University of Catania, Italy).

Supported by grants from the European Union – Fondi Europei per lo Sviluppo Regionale, Italian Ministero dell'Istruzione e dell'Università and Italian Ministero dello Sviluppo Economico (PON01 02464; Roma, Italy).

Disclosure: **C. Motta**, None; **G. Lupo**, None; **D. Rusciano**, None; **M. Olivieri**, None; **L. Lista**, None; **M. De Rosa**, P; **V. Pavone**, P; **C.D. Anfuso**, None

References

1. Folkman J. Tumor angiogenesis: therapeutic implications. *N Engl J Med*. 1971;285:1182–1186.
2. Carmeliet P, Jain RK. Angiogenesis in cancer and other diseases. *Nature*. 2000;407:249–257.
3. Congdon N, O'Colmain B, Klaver CC, et al. Causes and prevalence of visual impairment among adults in the United States. *Arch Ophthalmol*. 2004;122:477–485.
4. Klein BE. Overview of epidemiologic studies of diabetic retinopathy. *Ophthalmic Epidemiol*. 2007;14:179–183.
5. Semeraro F, Parrinello G, Cancarini A, et al. Predicting the risk of diabetic retinopathy in type 2 diabetic patients. *J Diabetes Complicat*. 2011;25:292–297.
6. Friedman DS, O'Colmain BJ, Munoz B, et al. Prevalence of age-related macular degeneration in the United States. *Arch Ophthalmol*. 2004;122:564–572.
7. Chen J, Stahl A, Hellstrom A, Smith LE. Current update on retinopathy of prematurity: screening and treatment. *Curr Opin Pediatr*. 2011;23:173–178.
8. Albert DM, Tapper D, Robinson NL, Felman R. Retinoblastoma and angiogenesis activity. *Retina*. 1984;4:189–194.
9. Shan GY, Zhang JH, Lü YG, Yun J. Bioinformatics-led design of single-chain antibody molecules targeting DNA sequences for retinoblastoma. *Int J Ophthalmol*. 2011;4:8–13.
10. Adamis AP, Shima DT. The role of vascular endothelial growth factor in ocular health and disease. *Retina*. 2005;25:111–118.
11. Lupo G, Motta C, Salmeri M, Spina-Purrello V, Alberghina M, Anfuso CD. An in vitro retinoblastoma human triple culture model of angiogenesis: a modulatory effect of TGF-β. *Cancer Lett*. 2014;354:181–188.

12. Andreoli CM, Miller JW. Anti-vascular endothelial growth factor therapy for ocular neovascular disease. *Curr Opin Ophthalmol*. 2007;18:502–508.
13. Ploug M, Rønne E, Behrendt N, Jensen AL, Blasi F, Danø K. Cellular receptor for urokinase plasminogen activator. Carboxyl-terminal processing and membrane anchoring by glycosyl- phosphatidylinositol. *J Biol Chem*. 1991;266:1926–1933.
14. Blasi F, Carmeliet P. uPAR: a versatile signaling orchestrator. *Nat Rev Mol Cell Biol*. 2002;3:932–943.
15. Carriero MV, Stoppelli MP. The urokinase- type plasminogen activator and the generation of inhibitors of urokinase activity and signaling. *Curr Pharm Des*. 2011;17:1944–1961.
16. Binder BR, Mihaly J, Prager GW. uPAR-uPA-PAI-1 interactions and signaling: a vascular biologist's view. *Thromb Haemost*. 2007;97:336–342.
17. Selleri C, Montuori N, Ricci P, et al. Involvement of the urokinase type plasminogen activator receptor in hematopoietic stem cell mobilization. *Blood*. 2005;105:2198–2205.
18. McGuire PG, Jones TR, Talarico N, Warren E, Das A. The urokinase/urokinase receptor system in retinal neovascularization: inhibition by A6 suggests a new therapeutic target. *Invest Ophthalmol Vis Sci*. 2003;44:2736–2742.
19. Sugioka K, Kodama A, Okada K, et al. TGF-β2 promotes RPE cell invasion into a collagen gel by mediating urokinase-type plasminogen activator (uPA) expression. *Exp Eye Res*. 2013;115:13–21
20. Navaratna D, Menicucci G, Maestas J, Srinivasan R, McGuire P, Das A. A peptide inhibitor of the urokinase/urokinase receptor system inhibits alteration of the blood-retinal barrier in diabetes. *FASEB J*. 2008;22:3310–3317.
21. Bifulco K, Longanesi-Cattani I, Gala M, et al. The soluble form of urokinase receptor promotes angiogenesis through its ^{88}Ser-Arg-Ser-Arg-Tyr^{92} chemotactic sequence. *J Thromb Haemost*. 2010;8:2789–2799.
22. Bifulco K, Longanesi-Cattani I, Gargiulo L, et al. An urokinase receptor antagonist that inhibits cell migration by blocking the formyl peptide receptor. *FEBS Lett*. 2008;582:1141–1146.
23. Carriero MV, Longanesi-Cattani I, Bifulco K, et al. Structure-based design of an urokinase-type plasminogen activator receptor-derived peptide inhibiting cell migration and lung metastasis. *Mol Cancer Ther*. 2009;8:2708–2717.
24. Carriero MV, Bifulco K, Minopoli M, et al. UPARANT: a urokinase receptor-derived peptide inhibitor of VEGF-driven angiogenesis with enhanced stability and in vitro and in vivo potency. *Mol Cancer Ther*. 2014;13:1092–1104.
25. Dal Monte M, Rezzola S, Cammalleri M, et al. Antiangiogenic effectiveness of the urokinase receptor-derived peptide UPARANT in a model of oxygen-induced retinopathy. *Invest Ophthalmol Vis Sci*. 2015;56:2392–2407.
26. Cammalleri M, Dal Monte M, Locri F, et al. The urokinase receptor-derived peptide 1 Uparant mitigates angiogenesis in a mouse model of laser-induced choroidal neovascularization. *Invest Ophthalmol Vis Sci*. 2016;57:2586–2587.
27. Lupo G, Anfuso CD, Assero G, et al. Amyloid β(1-42) and its β(25-35) fragment induce in vitro phosphatidylcholine hydrolysis in bovine retina capillary pericytes. *Neurosci Lett*. 2001;303:185–188.
28. Lupo G, Nicotra A, Giurdanella G, et al. Activation of phospholipase A_2 and MAP kinases by oxidized low-density lipoproteins in immortalized GP8.39 endothelial cells. *Biochim Biophys Acta*. 2005;1735:135–150.
29. Anfuso CD, Lupo G, Romeo L, et al. Endothelial cell-pericyte cocultures induce PLA_2 protein expression through activation of PKC-alpha and the MAPK/ERK cascade. *J Lipid Res*. 2007;48:782–793.
30. Giurdanella G, Anfuso CD, Olivieri M, et al. Aflibercept, bevacizumab and ranibizumab prevent glucose-induced damage in human retinal pericytes in vitro through a PLA_2/COX-2/VEGF-A pathway. *Biochem Pharmacol*. 2015;96:278–287.
31. Weigand M, Hantel P, Kreienberg R, Waltenberger J. Autocrine vascular endothelial growth factor signaling in breast cancer. Evidence from cell lines and primary breast cancer cultures in vitro. *Angiogenesis*. 2005;8:197–204.
32. Steiner H, Berger AP, Godoy-Tundidor S, et al. An autocrine loop for vascular endothelial growth factor is established in prostate cancer cells generated after prolonged treatment with interleukin 6. *Eur J Cancer*. 2004;40:1066–1072.
33. Olsson AK, Dimberg A, Kreuger J, Claesson-Welsh L. VEGF receptor signaling in control of vascular function. *Nat Rev Mol Cell Biol*. 2006;7:359–371.
34. Jung JE, Lee HG, Cho IH, et al. STAT3 is a potential modulator of HIF-1-mediated VEGF expression in human renal carcinoma cells. *FASEB J*. 2005;19:1296–1298.
35. Bartoli M, Platt D, Lemtalsi T, et al. VEGF differentially activates STAT3 in microvascular endothelial cells. *FASEB J*. 2003;17:1562–1564.
36. Osaadon P, Fagan XJ, Lifshitz T, Levy J. A review of anti-VEGF agents for proliferative diabetic retinopathy. *Eye (Lond)*. 2014;28:510–520.
37. Prevete N, Liotti F, Marone G, Melillo RM, de Paulis A. Formyl peptide receptors at the interface of inflammation, angiogenesis and tumor growth. *Pharmacol Res*. 2015;102:184–191.
38. Breuss JM, Uhrin P. VEGF-initiated angiogenesis and the uPA/uPAR system. *Cell Adh Migr*. 2012;6:535–615.
39. Uhrin P, Breuss JM. uPAR A modulator of VEGF-induced angiogenesis. *Cell Adh Migr*. 2013;7:23–26.
40. Prager GW, Breuss JM, Steurer S, et al. Vascular endothelial growth factor receptor-2-induced initial endothelial cell migration depends on the presence of the urokinase receptor. *Circ Res*. 2004;94:1562–1570.
41. Giebel SJ, Menicucci G, McGuire PG, Das A. Matrix metalloproteinase in early diabetic retinopathy and their role in alteration of the blood-retinal barrier. *Lab Invest*. 2005;85:597–607.
42. Cai J, Jiang WG, Ahmed A, Boulton M. Vascular endothelial growth factor-induced endothelial cell proliferation is regulated by interaction between VEGFR-2, SH-PTP1 and eNOS. *Microvasc Res*. 2006;71:20–31.
43. Niu G, Wright KL, Huang M, et al. Constitutive Stat3 activity up-regulates VEGF expression and tumor angiogenesis. *Oncogene*. 2002;21:2000–2008.
44. Carbajo-Pescador S, Ordoñez R, Benet M, et al. Inhibition of VEGF expression through blockade of HIF1α and STAT3 signaling mediates the anti-angiogenic effect of melatonin in HepG2 liver cancer cells. *Br J Cancer*. 2013;109:83–91.
45. Levy DE, Lee CK. What does Stat3 do? *J Clin Invest*. 2002;109:1143–1148.
46. Choi JH, Ahn MJ, Park CK, et al. Phospho-Stat3 expression and correlation with VEGF, p53, and Bcl-2 in gastric carcinoma using tissue microarray. *APMIS*. 2006;114:619–625.
47. Chen SH, Murphy DA, Lassoued W, Thurston G, Feldman MD, Lee WM. Activated STAT3 is a mediator and biomarker of VEGF endothelial activation. *Cancer Biol Ther*. 2008;7:1994–2003.
48. Wang H, Yang Z, Jiang Y, Hartnett ME. Endothelial NADPH oxidase 4 mediates vascular endothelial growth factor receptor 2-induced intravitreal neovascularization in a rat model of retinopathy of prematurity. *Mol Vis*. 2014;20:231–241.
49. Yadav UC, Srivastava SK, Ramana KV. Prevention of VEGF-induced growth and tube formation in human retinal endothelial cells by aldose reductase inhibition. *J Diabetes Complications*. 2012;26:369–377.

Investigative Ophthalmology & Visual Science

50. Jin YJ, Park I, Hong IK, et al. Fibronectin and vitronectin induce AP-1-mediated matrix metalloproteinase-9 expression through integrin α(5)/β(1)- and α(v)/β(3)-dependent Akt ERK and JNK signaling pathways in human umbilical vein endothelial cells. *Cell Signal*. 2011;23:125–134.
51. Hwang YP, Yun HJ, Choi JH, et al. Suppression of EGF-induced tumor cell migration and matrix metalloproteinase-9 expression by capsaicin via the inhibition of EGFR-mediated FAK/Akt, PKC/Raf/ERK, p38 MAPK, and AP-1 signaling. *Mol Nutr Food Res*. 2011;55:594–605.
52. Yang J, Caldwell RB, Behzadian MA. Blockade of VEGF-induced GSK/β-catenin signaling, uPAR expression and increased permeability by dominant negative p38α. *Exp Eye Res*. 2012; 100:101–108.

Investigative Ophthalmology & Visual Science